

USM-TH-123

On Lepton Flavor Violation in Tau Decays

G. Cvetič^{1*}, C. Dib^{1†}, C. S. Kim^{2‡}, and J. D. Kim^{2§}

¹*Department of Physics, Universidad Técnica Federico Santa María, Valparaíso, Chile*

²*Department of Physics and IPAP, Yonsei University, Seoul 120-749, Korea*

May 20, 2019

Abstract

We study lepton flavor violation (LFV) in tau decays induced by heavy Majorana neutrinos within two models: (I) the Standard Model with additional right-handed heavy Majorana neutrinos, i.e., a typical seesaw-type model; (II) the Standard Model with left-handed and right-handed neutral singlets, which are inspired by certain scenarios of $SO(10)$ models and heterotic superstring models with E_6 symmetry. We calculate various LFV branching ratios and a T-odd asymmetry. The seesaw Model I predicts very small branching ratios for LFV processes in most of the parameter space, but it can reach maximal branching ratios $Br(\tau \rightarrow \mu\gamma) \sim 10^{-10}$ and $Br(\tau \rightarrow 3\mu) \sim 10^{-11}$ in a very restricted parameter region. In contrast, Model II may show large enough branching ratios $Br(\tau \rightarrow e\gamma) \sim 10^{-8}$ and $Br(\tau \rightarrow 3e) \lesssim 10^{-9}$ to be tested by experiments in the near future.

*cvetic@fis.utfsm.cl

†cdib@fis.utfsm.cl

‡cskim@yonsei.ac.kr

§jdkim@phya.yonsei.ac.kr

I. INTRODUCTION

One of the many puzzles remaining in the current phenomenology of particle physics is to understand the smallness of the masses ($\lesssim 1$ eV) of standard neutrinos ν_e , ν_μ and ν_τ , compared to those of charged leptons. If neutrinos are of a Dirac nature, nonzero masses could be obtained in the Standard Model (SM) by introduction of a sterile right-handed neutrino. On the other hand, if neutrinos have a Majorana nature, more appealing solutions to the small neutrino mass problem exist. In order to avoid the explicit breaking of the SM gauge symmetry and still obtain nonzero Majorana mass terms (via spontaneous symmetry breaking), an additional Higgs triplet is needed in the SM. The latter would result in physical Nambu–Goldstones, but these have been excluded by experiments at LEP. On the other hand, various models in the context of extended gauge structures result in Majorana mass terms and could give possible solutions to the neutrino mass problem. An appealing solution is the seesaw mechanism [1] within the framework of $SO(10)$ or left–right symmetric models. In the conventional seesaw models, the effective light neutrino masses are within the scales of eV and MeV via a relation involving the hierarchy between very large Majorana masses and the Dirac masses at the electroweak scale. Another possible solution was investigated in the framework of heterotic superstring models [2] with E_6 symmetry or certain scenarios of $SO(10)$ models [3], where the low–energy effective theories include new left–handed and right–handed neutral isosinglets and assume conservation of total lepton number in the Yukawa sector.

One possibility to test the neutrino sector lies in the study and measurement of lepton–flavor–violating (LFV) processes, e.g., $\mu \rightarrow e\gamma$ or $3e$; $\tau \rightarrow \mu\gamma$ or 3μ ; $\tau \rightarrow e\gamma$ or $3e$. Such processes are practically suppressed to zero in the SM, due to the unitarity of the leptonic analog of the CKM mixing matrix and the near masslessness of the three neutrinos. Motivated by the aforementioned models with an extended neutrino sector, the authors in Refs. [4–6] derived analytic expressions for LFV decay rates of charged leptons in such models with heavy Majorana neutrinos. The authors of Ref. [7] gave a model–independent framework for analyzing $\mu \rightarrow e\gamma$ and $\mu \rightarrow 3e$ processes and investigated specific features of several Supersymmetric GUTs. They focused on Parity– and T–violating asymmetries involving muon polarization in the initial state.

Some generic properties of LFV processes and the corresponding constraints on the neutrino mass matrix have been studied in Ref. [8]. Phenomenological studies of various LFV and lepton–number–violating processes have appeared in the literature, including direct production of heavy Majorana neutrinos at various colliders [9], heavy Majorana mediated processes [10], and LFV processes (including $\mu \rightarrow e\gamma$ and $\tau \rightarrow \mu\gamma$) in supersymmetric frameworks [11].

In this paper we will consider LFV decays of tau leptons in the framework of the two aforementioned models with extended neutrino sectors. We will concentrate on the calculation of the corresponding LFV branching ratios and the corresponding expected numbers

of events. In addition, we will calculate a T-odd asymmetry induced by these processes.¹ In Sec. II we review the two models in question. In Sec. III we present the formulas for the branching ratios of charged lepton decays, $l \rightarrow l'\gamma$ and $l \rightarrow 3l'$, and the T-odd asymmetry within these two models. In Sec. IV we present numerical estimates for LFV tau decays, exploring the possibility of obtaining sizable rates that can be measured in the foreseeable future, yet keeping consistency with present experimental constraints. We give a summary and state our conclusions in Sec. V.

II. TWO SEESAW-TYPE MODELS

To set up our notation, we briefly review the two models considered in Ref. [4]: We call *Model I* the SM with the addition of right-handed neutrinos (singlets under the gauge group) and with the seesaw mechanism involved, and *Model II* the SM with both left-handed and right-handed neutral singlets.

In Model I, there is a number N_R of right-handed neutrinos, ν_{Ri} , in addition to the N_L standard left-handed neutrinos ν_{Li} (N_L also stands for the number of generations in the SM). The Yukawa interaction containing the neutrino masses (after gauge symmetry breaking) is written as

$$-\mathcal{L}_Y^\nu = \frac{1}{2} \left(\bar{\nu}_L, \bar{\nu}_R^c \right) \mathcal{M} \begin{pmatrix} \nu_L^c \\ \nu_R \end{pmatrix} + h.c., \quad (1)$$

where the $(N_L + N_R) \times (N_L + N_R)$ dimensional neutrino mass matrix has the seesaw block form [1]

$$\mathcal{M} = \begin{pmatrix} 0 & m_D \\ m_D^T & m_M \end{pmatrix} \quad (2)$$

and can always be diagonalized with a congruent transformation:

$$U \mathcal{M} U^T = \hat{\mathcal{M}}, \quad (3)$$

where U is a unitary matrix. The mass eigenstates are a total of $N_L + N_R$ Majorana neutrinos, n_i , related to the original ones ν_a by the matrix U :

$$\begin{pmatrix} \nu_L \\ \nu_R^c \end{pmatrix}_a = \sum_{i=1}^{N_L+N_R} U_{ia}^* n_{Li}, \quad \begin{pmatrix} \nu_L^c \\ \nu_R \end{pmatrix}_a = \sum_{i=1}^{N_L+N_R} U_{ia} n_{Ri}. \quad (4)$$

¹ Under the assumption of CPT symmetry, CP violation is equivalent to T violation. While standard CP violation appears in the quark sector, it could also arise, for example, in processes which involve only elementary (SM) bosons [12] or (heavy) Majorana neutrinos [13,14].

The first N_L mass eigenstates (n_ℓ , $\ell = 1, \dots, N_L$) are light and are identified with the standard partners of the charged leptons, while the remaining N_R mass eigenstates (n_h , $h = N_L + 1, \dots, N_L + N_R$) are heavy Majorana neutrinos.

As notation, we will consistently use the indices a, b, c to refer to *all* interaction eigenstates ν_a (both standard and extra neutrinos), while to explicitly indicate *the standard interaction eigenstates*, we use the index l (lepton flavor). Similarly, we will use i, j, k to refer to *all* mass eigenstates n_i , while the index ℓ (as in n_ℓ) will indicate the first N_L (light) neutrinos, and the index h (as in n_h) the remaining (heavy) neutrinos.

We can then construct the interaction Lagrangian for leptons (including the Majorana neutrinos) and gauge bosons (W^\pm and Z). Ref. [4] introduced a $N_L \times (N_L + N_R)$ -dimensional matrix B of charged current interaction coefficients, and a $(N_L + N_R) \times (N_L + N_R)$ -dimensional matrix C of neutral current interaction coefficients, respectively defined as

$$B_{li} = U_{il}^*, \quad C_{ij} = \sum_{a=1}^{N_L} U_{ia} U_{ja}^*, \quad (5)$$

where the charged leptons are taken in their mass basis. In this model, the ratio between the Dirac mass (m_D) and the Majorana mass (m_M) characterizes the strength of the heavy-to-light neutrino mixings ($s_L^{\nu_l}$) $^2 \equiv \sum_h |U_{hl}|^2$ ($\sim |m_D|^2/|m_M|^2$), as well as the size of the physical light neutrino masses:

$$m_{\nu_{light}} \sim m_D^2/m_M. \quad (6)$$

In this model, it is the very low experimental bounds on $m_{\nu_{light}}$ ($\lesssim 1$ eV) which impose severe constraints on the $|m_D| \ll |m_M|$ hierarchy required, and consequently also on the heavy-to-light neutrino mixings.

Alternatively, Model II contains an equal number N_R of left-handed neutral singlets, S_{Li} , as well as right-handed neutrinos, ν_{Ri} [2,3], where we assume that $\Delta L = 2$ interactions are absent. After the electroweak symmetry breaking, the Yukawa sector relevant for the neutrino masses can be written as

$$-\mathcal{L}_Y^\nu = \frac{1}{2} (\bar{\nu}_L, \bar{\nu}_R^c, \bar{S}_L) \mathcal{M} \begin{pmatrix} \nu_L^c \\ \nu_R \\ S_L^c \end{pmatrix} + h.c., \quad (7)$$

where the $(N_L + 2N_R) \times (N_L + 2N_R)$ neutrino mass matrix has the form

$$\mathcal{M} = \begin{pmatrix} 0 & m_D & 0 \\ m_D^T & 0 & m_M^T \\ 0 & m_M & 0 \end{pmatrix}. \quad (8)$$

This model predicts, for each generation, a massless Weyl neutrino, and two degenerate neutral Majorana neutrinos. Consequently, the seesaw-type restriction in Eq. (6), imposed

by the light neutrinos within the previous model, does not apply here [15,16]. In Model II, it is not the smallness of light neutrino masses but the present experimental bounds on the heavy-to-light mixing parameters $(s_L^{\nu_l})^2 \sim |m_D|^2/|m_M|^2$ ($\lesssim 10^{-2}$, see later) which imposes a certain level of hierarchy $|m_D| < |m_M|$ between the Dirac and Majorana mass sector. This hierarchy is in general much weaker than in the seesaw-type models. Although this simple model features massless neutrinos in the light sector, nonzero masses for the light neutrinos can still be generated by introducing small perturbations in the lower right block of \mathcal{M} [Eq. (8)], which corresponds to small Majorana mass terms for the neutral singlets S_{Li} , without much effect on the mixings.

III. FLAVOR-VIOLATING TAU DECAYS WITHIN THESE MODELS

Recently LFV processes have been investigated extensively because SUSY GUTs predict that the branching ratios for $\mu \rightarrow e\gamma$ and $\mu \rightarrow 3e$ and the $\mu - e$ conversion rate in a nucleus can reach just below present experimental bounds [7,17]. Here we address the predictions for LFV decays of the form $l \rightarrow l'\gamma$ and $l \rightarrow 3l'$ within the models of Section II.

We can find the amplitudes for $l \rightarrow l'\gamma$ and $l \rightarrow 3l'$ in terms of our model parameters. These processes occur only at one loop level or higher in the (extended) electroweak theory. The amplitude for $l \rightarrow l'\gamma$ (a γ -penguin with the photon on the mass shell) is

$$\mathcal{M}(l \rightarrow l'\gamma) = i \frac{e\alpha_w}{8\pi M_W^2} \epsilon^\mu \sum_{i=1}^{N_L + \tilde{N}_R} B_{li}^* B_{l'i} G_\gamma(\lambda_i) \bar{u}_{l'} i\sigma_{\mu\nu} q^\nu (m_{l'} P_L + m_l P_R) u_l , \quad (9)$$

where ϵ^μ is the photon polarization and $\lambda_i = m_i^2/M_W^2$, are the squared neutrino masses inside the loop, in units of M_W ($G_\gamma(x)$ is a loop function given below). We have denoted N_R in Model I and $2N_R$ in Model II generically as \tilde{N}_R .

The amplitude for $l \rightarrow 3l'$ receives contributions from γ -penguins, Z -penguins and box diagrams, namely [4]:

$$\begin{aligned} \mathcal{M}_\gamma(l \rightarrow 3l') = & -i \frac{\alpha_w^2 s_w^2}{2M_W^2} \sum_{i=1}^{N_L + \tilde{N}_R} B_{li}^* B_{l'i} \bar{u}_{l'} \gamma^\mu v_{l'} \bar{u}_{l'} \left[F_\gamma(\lambda_i) \left(\gamma_\mu - \frac{q_\mu q_\nu \gamma^\nu}{q^2} \right) P_L \right. \\ & \left. - G_\gamma(\lambda_i) i\sigma_{\mu\nu} \frac{q^\nu}{q^2} (m_{l'} P_L + m_l P_R) \right] u_l , \end{aligned} \quad (10)$$

$$\begin{aligned} \mathcal{M}_Z(l \rightarrow 3l') = & -i \frac{\alpha_w^2}{8M_W^2} \bar{u}_{l'} \gamma_\mu P_L u_l \bar{u}_{l'} \gamma^\mu \left[(2 - 4s_w^2) P_L - 4s_w^2 P_R \right] v_{l'} \\ & \times \sum_{i,j=1}^{N_L + \tilde{N}_R} B_{li}^* B_{l'j} \left[\delta_{ij} F_Z(\lambda_i) + C_{ij} H_Z(\lambda_i, \lambda_j) + C_{ij}^* G_Z(\lambda_i, \lambda_j) \right] , \end{aligned} \quad (11)$$

$$\mathcal{M}_{Box}(l \rightarrow 3l') = -i \frac{\alpha_w^2}{4M_W^2} \bar{u}_{l'} \gamma_\mu P_L u_l \bar{u}_{l'} \gamma^\mu P_L v_{l'} \quad (12)$$

$$\times \sum_{i,j=1}^{N_L+\tilde{N}_R} \left[2B_{l'i}B_{l'j}B_{li}^*B_{l'j}^* F_{Box}(\lambda_i, \lambda_j) + B_{l'i}B_{l'i}B_{lj}^*B_{l'j}^* G_{Box}(\lambda_i, \lambda_j) \right], \quad (12)$$

The loop functions that appear in these expressions have the following explicit forms:

$$F_\gamma(x) = \frac{7x^3 - x^2 - 12x}{12(1-x)^3} - \frac{x^4 - 10x^3 + 12x^2}{6(1-x)^4} \ln x, \quad (13)$$

$$G_\gamma(x) = -\frac{2x^3 + 5x^2 - x}{4(1-x)^3} - \frac{3x^3}{2(1-x)^4} \ln x, \quad (14)$$

$$F_Z(x) = -\frac{5x}{2(1-x)} - \frac{5x^2}{2(1-x)^2} \ln x, \quad (15)$$

$$G_Z(x, y) = -\frac{1}{2(x-y)} \left[\frac{x^2(1-y)}{1-x} \ln x - \frac{y^2(1-x)}{1-y} \ln y \right], \quad (16)$$

$$H_Z(x, y) = \frac{\sqrt{xy}}{4(x-y)} \left[\frac{x^2 - 4x}{1-x} \ln x - \frac{y^2 - 4y}{1-y} \ln y \right], \quad (17)$$

$$\begin{aligned} F_{Box}(x, y) = & \frac{1}{x-y} \left[(1 + \frac{xy}{4}) \left(\frac{1}{1-x} + \frac{x^2 \ln x}{(1-x)^2} - \frac{1}{1-y} - \frac{y^2 \ln y}{(1-y)^2} \right) \right. \\ & \left. - 2xy \left(\frac{1}{1-x} + \frac{x \ln x}{(1-x)^2} - \frac{1}{1-y} - \frac{y \ln y}{(1-y)^2} \right) \right], \end{aligned} \quad (18)$$

$$\begin{aligned} G_{Box}(x, y) = & -\frac{\sqrt{xy}}{x-y} \left[(4 + xy) \left(\frac{1}{1-x} + \frac{x \ln x}{(1-x)^2} - \frac{1}{1-y} - \frac{y \ln y}{(1-y)^2} \right) \right. \\ & \left. - 2 \left(\frac{1}{1-x} + \frac{x^2 \ln x}{(1-x)^2} - \frac{1}{1-y} - \frac{y^2 \ln y}{(1-y)^2} \right) \right]. \end{aligned} \quad (19)$$

It is convenient to abbreviate the combinations of mixing elements and loop functions that appear in the amplitudes as:

$$F_\gamma^{ll'} = \sum_{i=1}^{N_L+\tilde{N}_R} B_{li}^* B_{l'i} F_\gamma(\lambda_i), \quad (20)$$

$$F_Z^{ll'} = \sum_{i,j=1}^{N_L+\tilde{N}_R} B_{li}^* B_{l'j} \left[\delta_{ij} F_Z(\lambda_i) + C_{ij} H_Z(\lambda_i, \lambda_j) + C_{ij}^* G_Z(\lambda_i, \lambda_j) \right], \quad (21)$$

$$F_{Box}^{ll'} = \sum_{i,j=1}^{N_L+\tilde{N}_R} \left[2B_{l'i}B_{l'j}B_{li}^*B_{l'j}^* F_{Box}(\lambda_i, \lambda_j) + B_{l'i}B_{l'i}B_{lj}^*B_{l'j}^* G_{Box}(\lambda_i, \lambda_j) \right], \quad (22)$$

$$G_\gamma^{ll'} = \sum_{i=1}^{N_L+\tilde{N}_R} B_{li}^* B_{l'i} G_\gamma(\lambda_i), \quad (23)$$

Now, the most general effective Lagrangian for the processes $l \rightarrow l'\gamma$ and $l \rightarrow 3l'$ is:

$$\mathcal{L} = -\frac{4G_F}{\sqrt{2}} \{ A_R m_l \bar{l}_R \sigma^{\mu\nu} l'_L F_{\mu\nu} + A_L m_l \bar{l}_L \sigma^{\mu\nu} l'_R F_{\mu\nu}$$

$$\begin{aligned}
& + g_1 (\bar{l}_R l'_L) (\bar{l}'_R l'_L) + g_2 (\bar{l}_L l'_R) (\bar{l}'_L l'_R) \\
& + g_3 (\bar{l}_R \gamma^\mu l'_R) (\bar{l}'_R \gamma^\mu l'_R) + g_4 (\bar{l}_L \gamma^\mu l'_L) (\bar{l}'_L \gamma^\mu l'_L) \\
& + g_5 (\bar{l}_R \gamma^\mu l'_R) (\bar{l}'_L \gamma^\mu l'_L) + g_6 (\bar{l}_L \gamma^\mu l'_L) (\bar{l}'_R \gamma^\mu l'_R) \\
& + h.c. \}, \tag{24}
\end{aligned}$$

where G_F is the Fermi coupling constant, the subindices R and L refer to fermion chirality (projected by $(1 + \gamma_5)/2$ and $(1 - \gamma_5)/2$ respectively), A_R and A_L are dimensionless electromagnetic penguin coupling constants, while g_i , ($i = 1, \dots, 6$) are dimensionless four-fermion coupling constants. Processes with real photons like $l \rightarrow l' \gamma$ receive contributions from A_R and A_L only, while $l \rightarrow 3l'$ receive contributions from all of the couplings above.

All of these couplings are in general complex numbers and calculable in lepton flavor violating models. In the case of our models, we have:

$$g_1 = g_2 = g_3 = g_5 = 0, \tag{25}$$

$$g_4 = \frac{\alpha_w}{8\pi} \{ 2s_w^2 F_\gamma^{ll'} + (1 - 2s_w^2) F_Z^{ll'} + F_{Box}^{ll'} \}, \tag{26}$$

$$g_6 = \frac{\alpha_w}{8\pi} \{ 2s_w^2 F_\gamma^{ll'} + (-2s_w^2) F_Z^{ll'} \}, \tag{27}$$

$$eA_R = \frac{\alpha}{8\pi} G_\gamma^{ll'}, \tag{28}$$

$$eA_L = \frac{\alpha}{8\pi} G_\gamma^{ll'} \frac{m_{l'}}{m_l}, \tag{29}$$

where $\alpha_w = g_2^2/(4\pi) \approx 0.0339$, $\alpha = e_0^2/(4\pi)$. In terms of these couplings, the decay rate for $l \rightarrow l' \gamma$ was calculated in Ref. [7] as

$$\Gamma(l \rightarrow l' \gamma) = \Gamma(l \rightarrow e\bar{\nu}_e \nu_l) \cdot 384\pi^2 (|A_R|^2 + |A_L|^2). \tag{30}$$

Similarly, the integrated decay rate for $l \rightarrow 3l'$, with a cut Δ in the final phase space (see below), is also found in Ref. [7]:

$$\begin{aligned}
\Gamma(l \rightarrow 3l')[\Delta] = & \Gamma(l \rightarrow e\bar{\nu}_e \nu_l) \cdot 3 \left\{ \left(\frac{|g_1|^2 + |g_2|^2}{16} + |g_3|^2 + |g_4|^2 \right) I_1[\Delta] \right. \\
& + \left(|g_5|^2 + |g_6|^2 \right) I_2[\Delta] + \left(|eA_R|^2 + |eA_L|^2 \right) I_3[\Delta] \\
& \left. + Re(eA_R g_4^* + eA_L g_3^*) I_4[\Delta] + Re(eA_R g_6^* + eA_L g_5^*) I_5[\Delta] \right\}, \tag{31}
\end{aligned}$$

where

$$I_1[\Delta] = \frac{2}{3} (1 + 2\Delta)(1 - 2\Delta)^3, \tag{32}$$

$$I_2[\Delta] = \frac{1}{3} (1 + 2\Delta - 2\Delta^2)(1 - 2\Delta)^2, \tag{33}$$

$$I_3[\Delta] = \frac{16}{3}(1-\Delta)(2-\Delta+2\Delta^2) \ln \frac{1-\Delta}{\Delta} - \frac{8}{9}(1-2\Delta)(13-4\Delta+4\Delta^2), \quad (34)$$

$$I_4[\Delta] = \frac{16}{3}(1-2\Delta)^3, \quad (35)$$

$$I_5[\Delta] = \frac{8}{3}(1+\Delta)(1-2\Delta)^2. \quad (36)$$

The cut Δ (< 1), which was introduced to optimize a T-odd asymmetry A_T (explained below) and should be fixed after analyzing the actual experimental distribution in the Dalitz plot, is defined as follows. Let E_1 be the energy of one of the final leptons in a given event, m_l the mass of the decaying lepton and $m_{l'}$ the mass of any of the final leptons. Then the full range for E_1 is:

$$m_{l'} < E_1 < \left(1 - 3\frac{m_{l'}^2}{m_l^2}\right) \frac{m_l}{2}. \quad (37)$$

One then considers only the events in a kinematic range below certain energy $E_1 < (1-\Delta)m_l/2$, (with $\Delta > 3m_{l'}^2/m_l^2$), and chooses the value of Δ that maximizes the following T-odd asymmetry A_T in $l \rightarrow 3l'$ decays. In the numerical analysis, we found that the results are rather insensitive to the precise value of Δ , as long as it is of order $m_{l'}^2/m_l^2$.

A T-odd asymmetry can be defined in the decays $l \rightarrow 3l'$ which is sensitive to the CP phases of the neutrino mixing matrices, but has the experimental drawback that it requires independent knowledge of the initial lepton polarization (in this case, the tau lepton polarization). Defining, in the CM frame, the decay plane as the plane that contains the three final momenta, then A_T is the asymmetry between the cases when the polarization of the initial lepton points to one side or to the other side of the decay plane. Geometrically, A_T is a ϕ -angle asymmetry, where ϕ is the angle between the decay plane and the plane that contains the polarization vector of the initial lepton l and the momentum of the final lepton with charge opposite to l (see Ref. [7] for details). The explicit expression for A_T is then:

$$A_T = \frac{\int_0^\pi \frac{d\Gamma}{d\phi} d\phi - \int_\pi^{2\pi} \frac{d\Gamma}{d\phi} d\phi}{\Gamma} \quad (38)$$

and in terms of the effective lagrangian parameters is:

$$A_T[\Delta] = \frac{3\Gamma(l \rightarrow e\bar{\nu}_e\nu_l)}{2\Gamma(l \rightarrow 3l')[\Delta]} \left\{ Im\left(eA_R g_4^* + eA_L g_3^*\right) K_3[\Delta] - Im\left(eA_R g_6^* + eA_L g_5^*\right) K_4[\Delta] \right\}, \quad (39)$$

where

$$K_3[\Delta] = \frac{8}{105}\sqrt{1-2\Delta}(48-57\Delta-68\Delta^2+85\Delta^3) - 4(1-\Delta)^3 \sqrt{\Delta} \cos^{-1}\left(\frac{3\Delta-1}{1-\Delta}\right), \quad (40)$$

$$K_4[\Delta] = \frac{4}{105}\sqrt{1-2\Delta}(64-41\Delta+26\Delta^2-85\Delta^3) - 2(1-\Delta-\Delta^2+\Delta^3)\sqrt{\Delta} \cos^{-1}\left(\frac{3\Delta-1}{1-\Delta}\right). \quad (41)$$

IV. NUMERICAL RESULTS AND DISCUSSIONS

Severe constraints may come from data on neutrino flavor oscillations and the present bound on the electron neutrino mass $m_{\nu_e} < 3$ eV from tritium beta decay. The solar neutrino anomaly can be interpreted either by matter enhanced neutrino oscillations if $\Delta m_{sol}^2 \sim 1 \times 10^{-5}$ eV² with small or large mixing, or by vacuum oscillations if $\Delta m_{sol}^2 \sim 10^{-10}$ eV² with maximal mixing. The atmospheric neutrino experimental data shows evidence for $\Delta m_{atm}^2 \sim 2.2 \times 10^{-3}$ eV² with maximal mixing. We will assume that $\Delta m_{sol}^2 = |m_{\nu_\mu}^2 - m_{\nu_e}^2|$ and $\Delta m_{atm}^2 = |m_{\nu_\tau}^2 - m_{\nu_\mu}^2|$. Since $\Delta m_{sol}^2 \ll \Delta m_{atm}^2$, we may also take $\Delta m_{atm}^2 = |m_{\nu_\tau}^2 - m_{\nu_e}^2|$. Since $\Delta m_{atm}^2 \ll 3^2$ eV², we have the following upper bounds for all three light neutrino masses: $m_{\nu_e}, m_{\nu_\mu}, m_{\nu_\tau} < 3$ eV. Ref. [18] investigated possible patterns of the Majorana neutrino mass matrix which are compatible with these results and the non-observation of neutrinoless double beta decay. In the models we are considering, a number of low-energy experiments set upper bounds on possible non-Standard-Model couplings, which are characterized in Refs. [4,19] as $(s_L^{\nu_l})^2 \equiv \sum_{n_h} |B_{lh}|^2$. A recent analysis [20] of bounds on the mixing parameters $(s_L^{\nu_l})^2$ ($l = e, \mu, \tau$) gives:

$$(s_L^{\nu_e})^2 < 0.0071, \quad (s_L^{\nu_\mu})^2 < 0.0014, \quad (s_L^{\nu_\tau})^2 < 0.033. \quad (42)$$

As the bound on $(s_L^{\nu_\mu})^2$ is tighter, LFV muon decays are consistently more suppressed than tau decays. We will therefore concentrate our numerical analysis on tau decays, although the analysis of muon decays follows in a similar way. We will study the consequences of these models on tau decay rates of forbidden modes and CP violating asymmetries, using the constraints in Eq. (42) as well as the atmospheric neutrino oscillation data, Δm_{atm}^2 and the current bound on m_{ν_e} , quoted above. To date, the experimental upper bounds on $\tau \rightarrow l\gamma$ and $\tau \rightarrow 3l$ are [21]:

$$Br(\tau^- \rightarrow \mu^- \gamma) < 1.1 \times 10^{-6}, \quad (43)$$

$$Br(\tau^- \rightarrow e^- \gamma) < 2.7 \times 10^{-6}, \quad (44)$$

$$Br(\tau^- \rightarrow \mu^- \mu^- \mu^+) < 1.9 \times 10^{-6}, \quad (45)$$

$$Br(\tau^- \rightarrow e^- e^- e^+) < 2.9 \times 10^{-6}. \quad (46)$$

It is then important to verify if the models we are considering, keeping consistency with the constraints, are able to predict values for these branching ratios that are close to their present bounds.

A. Model I

First, let us study Model I in the two-generation SM with an extension of two right-handed neutrinos. The structure of CP-violating phases in these types of models was studied in Ref. [13]. In the case of N generations, the leptonic charged current mixing matrix (or

Maki–Nakagawa–Sakata matrix) is a $N \times 2N$ complex matrix $U_{MNS} = B^*$ [see Eq. (5)]: it contains $N(N-1)$ independent phases, which are identified as $(N-1)(N-2)/2$ Dirac phases, $N-1$ Majorana phases in the light neutrino sector, and the remaining $N(N-1)/2$ phases. The latter arise from the mixing of light and heavy neutrinos, and are called *heavy* phases. The neutrino mass spectrum for $N=2$ consists of two light Majorana neutrinos (which are identified with two of the three known neutrinos) and two heavy Majoranas denoted by n_3 and n_4 . In this case, the charged current mixing matrix $U_{MNS} = B^*$ is a 2×4 complex matrix. Therefore, it has 8 real and 8 imaginary parameters. It also satisfies two general conditions: first, the unitarity condition $U_{MNS}(U_{MNS})^\dagger = 1_{2 \times 2}$, imposes 3 constraints for the real parts and 1 for the imaginary parts; second, the seesaw condition $U_{MNS} \hat{\mathcal{M}} U_{MNS}^T = 0_{2 \times 2}$ leads to 3 constraints for each the real and imaginary parts. Then, there remain 2 real parts and 4 phases. After absorbing 2 unphysical phases into the two charged lepton fields, we have 2 independent physical phases –one Majorana phase ($N-1 = 1$) and one heavy phase ($N(N-1)/2 = 1$).

Let us take the Dirac and Majorana submatrices [see Eq. (2)], for $N=2$, to be of the form:

$$m_D = \begin{pmatrix} a & b e^{i\delta_1} \\ c e^{i\delta_2} & d \end{pmatrix}, \quad m_M = \begin{pmatrix} M_1 & 0 \\ 0 & M_2 \end{pmatrix}, \quad (47)$$

where a, b, c, d are real. Two phases, δ_1 and δ_2 , parametrize the Majorana and heavy phase in the two-generation scheme. We can identify the Majorana and heavy phases defined in Ref. [13] after a suitable transformation of our parametrization. The 4×4 symmetric neutrino mass matrix \mathcal{M} can always be diagonalized by a unitary matrix U , in the form $U \mathcal{M} U^T = \mathcal{M}_{diag}$, where \mathcal{M}_{diag} is a diagonal matrix with real positive elements (see the appendix).

Typical seesaw models of this kind produce an effective light neutrino mass matrix $m_{\nu_{light}} \approx m_D m_M^{-1} m_D^T$ when $m_D \ll m_M$

$$m_{\nu_{light}} = \begin{bmatrix} \left(\frac{a^2}{M_1} + \frac{b^2}{M_2} e^{2i\delta_1} \right) & \left(\frac{ac}{M_1} e^{i\delta_2} + \frac{bd}{M_2} e^{i\delta_1} \right) \\ \left(\frac{ac}{M_1} e^{i\delta_2} + \frac{bd}{M_2} e^{i\delta_1} \right) & \left(\frac{c^2}{M_1} e^{2i\delta_2} + \frac{d^2}{M_2} \right) \end{bmatrix} \times (1 + \mathcal{O}(m_D^2 m_M^{-2})), \quad (48)$$

and lepton flavor violating couplings of order $m_D m_M^{-1}$. Therefore, the upper bound on the electron neutrino mass usually severely constrains the neutrino mass matrix as well as the coupling strengths. LFV processes thus tend to be very suppressed.

Let us estimate the usual size of these LFV processes, and their upper bounds. First, we demand $\nu_\mu - \nu_\tau$ mixing to be close to maximal, to be consistent with recent atmospheric neutrino deficit experiments [22]. The mixing matrix among the light neutrinos (*i.e.* the upper left part of U^\dagger in Eq. (4)) is approximately unitary, of the form:

$$V \approx \begin{pmatrix} \cos \theta & -\sin \theta \exp(-i\varepsilon) \\ \sin \theta \exp(i\varepsilon) & \cos \theta \end{pmatrix}, \quad (49)$$

where $\theta = \pi/4$ corresponds to maximal mixing, and ε is a CP phase, function of δ_1 and δ_2 . If we demand that the maximal mixing is obtained independently of the values M_1 and M_2 of the heavy Majorana sector, then this implies the following simple relations in the light Dirac sector: $a^2 = c^2$, $b^2 = d^2$, and $\delta_1 = \delta_2$. The value of δ ($\equiv \delta_1 = \delta_2$) can be restricted to lie in the range $-\pi/2 < \delta \leq \pi/2$. The eigenmasses of the two light neutrinos are then

$$m_{\nu_1, \nu_2} = \left| \left[\left(\frac{a^2}{M_1} \right)^2 + \left(\frac{b^2}{M_2} \right)^2 + 2 \frac{a^2}{M_1} \frac{b^2}{M_2} \cos(2\delta) \right]^{1/2} \pm \left(\frac{ac}{M_1} + \frac{bd}{M_2} \right) \right| , \quad (50)$$

the CP-violating parameter ε of Eq. (49) is

$$\tan \varepsilon = \tan \delta \times \frac{(a^2/M_1) - (b^2/M_2)}{(a^2/M_1) + (b^2/M_2)} , \quad (51)$$

and the heavy-to-light mixing parameters (42) $(s_L^{\nu_\mu})^2 \equiv \sum_{h=3}^4 |B_{\mu h}|^2$ and $(s_L^{\nu_\tau})^2 \equiv \sum_{h=3}^4 |B_{\tau h}|^2$ are

$$(s_L^{\nu_\mu})^2 = (s_L^{\nu_\tau})^2 = \frac{a^2}{M_1^2} + \frac{b^2}{M_2^2} (\equiv s_L^2) . \quad (52)$$

We should also take sensible values for M_1 and M_2 , namely above ≥ 100 GeV to be consistent with the non-observation of heavy neutrinos to date. We take the convention $M_2 \geq M_1$ (≥ 100 GeV).

We then distinguish two cases for the parameters: case 1) $a = \pm c$ and $b = \pm d$; case 2) $a = \pm c$ and $b = \mp d$.

1. Case 1 ($a = \pm c$ and $b = \pm d$): We obtain $m_{\nu_\tau} \geq (a^2/M_1 + b^2/M_2)$, and thus $s_L^2 \leq m_{\nu_\tau}/M_1 < 3\text{eV}/M_1 = 3 \times 10^{-11}$. Since the branching ratios $Br(\tau \rightarrow \mu\gamma)$ and $Br(\tau \rightarrow 3\mu)$ are approximately proportional to $(s_L^{\nu_\mu})^2 (s_L^{\nu_\tau})^2 (= s_L^4)$, this value for s_L^2 implies highly suppressed branching ratios: $Br(\tau \rightarrow \mu\gamma) \lesssim 10^{-23}$ and $Br(\tau \rightarrow 3\mu) \lesssim 10^{-24}$. The corresponding results for $Br(\mu \rightarrow e\gamma)$ and $Br(\mu \rightarrow 3e)$ are obtained when we multiply the above numbers by $1/0.174 = 5.75$ [where 0.174 is the branching ratio $Br(\tau \rightarrow \mu\bar{\nu}_\mu\nu_\tau)$]: $Br(\mu \rightarrow e\gamma) \lesssim 10^{-22}$ and $Br(\mu \rightarrow 3e) \lesssim 10^{-23}$. The latter values are still many orders below the respective present experimental bounds (10^{-11} and 10^{-12}).
2. Case 2 ($a = \pm c$ and $b = \mp d$): We obtain $m_{\nu_\tau} \geq 2|a^2/M_1 - b^2/M_2|$, where the equality is achieved only when $\delta = \pi/2$. In the latter case, $m_{\nu_\mu} = 0$, and $m_{\nu_\tau} = 2|a^2/M_1 - b^2/M_2| = (\Delta m_{atm}^2)^{1/2} \approx 0.047$ eV. This special case ($\delta = \pi/2$) thus allows us to avoid the suppression of $s_L^2 = (a^2/M_1^2 + b^2/M_2^2)$ while keeping a^2/M_1 extremely close to b^2/M_2 . The maximal allowed heavy-to-light mixing parameter s_L^2 can then be saturated $s_L^2 = (s_L^2)_{\max} = 0.0014$ [see Eq. (42)] by the choice of the following parameters of the Dirac matrix m_D :

$$a = c = M_1(s_L)_{\max}/\sqrt{1 + M_1/M_2}, \quad b = -d = a(1 \pm \eta)\sqrt{M_2/M_1}, \quad (53)$$

$$\eta = \sqrt{\Delta m_{\text{atm}}^2} \left(1 + \frac{M_1}{M_2}\right) \frac{1}{4M_1(s_L^2)_{\max}} \approx 1.17 \times 10^{-13} \times \frac{1}{(s_L^2)_{\max}} \left(1 + \frac{M_1}{M_2}\right), \quad (54)$$

where, as mentioned, $\delta = \pi/2$. The rates $\tau \rightarrow \mu\gamma$ and $\tau \rightarrow 3\mu$ are practically proportional to (s_L^4) and approximately reach their maximum (for fixed chosen values of M_1 and M_2) for the case (53)–(54), as shown in the Appendix. The conditions (53)–(54) give us the largest possible branching ratios in Model I, $Br(\tau \rightarrow \mu\gamma) \sim 10^{-10}$ and $Br(\tau \rightarrow \mu\mu\mu) \lesssim 10^{-11}$ (when $100 \text{ GeV} = M_1 \leq M_2 \leq 1000 \text{ GeV}$). In Fig. 1 we show the two branching ratios as function of M_2 by setting $M_1 = 100 \text{ GeV}$. The CP-violating asymmetry parameter A_T (39) is in this case, unfortunately, equal to zero, since $\delta = \pi/2$ implies $\varepsilon = 0$ (51) and thus no CP violation.

The above results refer to the case of the approximately minimal allowed value of M_1 ($M_1 = 100 \text{ GeV}$). The LFV branching ratios increase when M_1 increases and M_2/M_1 and s_L^2 are kept fixed. Stated otherwise, the mixing parameter value $(s_L)^2$ needed to achieve a certain value of the branching ratio decreases when M_1 increases (and M_2/M_1 is kept fixed). This is depicted in Figs. 2 and 3 for various fixed values of the $\tau \rightarrow \mu\gamma$ and $\tau \rightarrow 3\mu$ branching ratios, respectively.

Now, when we move the value of δ away from $\pi/2$, the allowed branching ratios drops sharply, mainly due to the required upper bounds $m_{\nu_\mu}, m_{\nu_\tau} < 3 \text{ eV}$, i.e. a situation similar to Case 1 sets in.

The corresponding results for $Br(\mu \rightarrow e\gamma)$ and $Br(\mu \rightarrow 3e)$ may again be obtained by multiplying the above numbers by $1/0.174 = 5.75$. However, in the case of the $\nu_\mu - \nu_e$ scenario, the mixing bounds (42) do not apply separately, but in a more restrictive form: $(s_L^{\nu_\mu})^2 \times (s_L^{\nu_e})^2 \lesssim 10^{-10}$, i.e., $s_L^2 \lesssim 10^{-5}$, and the branching ratios in the discussed “optimal” case 2 are lower: $Br(\mu \rightarrow e\gamma) < 10^{-13}$ and $Br(\mu \rightarrow 3e) < 10^{-14}$, which is at least two orders below the present respective experimental bounds (10^{-11} and 10^{-12}).

If we look at the processes $\tau \rightarrow e\gamma$ and $\tau \rightarrow eee$, the above analysis does not apply, because the experimental evidence indicates that in that case the mixing between ν_e and ν_τ is not nearly maximal, but nearly zero [$\theta \approx 0$ in Eq. (49)]. If we assume that the zero mixing condition is fulfilled independently of the heavy Majorana sector, then we obtain the relations $ac = 0$ and $bd = 0$. The cases $a = b = 0$ and $c = d = 0$ give us $(s_L^{\nu_e})^2 = 0$ and $(s_L^{\nu_\tau})^2 = 0$, respectively, and thus extremely suppressed branching ratios. The cases $a = d = 0$ and $b = c = 0$ give also very suppressed mixing parameters: $(s_L^{\nu_e})^2 (s_L^{\nu_\tau})^2 < m_\nu/M_1 < 3 \text{ eV}/100 \text{ GeV} = 3 \times 10^{-11}$, i.e., as in the afore-discussed case 1 we obtain extremely suppressed branching ratios.

B. Model II

Now let us consider Model II in a two-generation scheme, where the neutrino mass matrix has the form of Eq. (8). For the 2×2 submatrices m_D and m_M , we take:

$$m_D = \begin{pmatrix} a & be^{i\xi} \\ ce^{i\xi} & d \end{pmatrix}, \quad m_M = \begin{pmatrix} M_1 & 0 \\ 0 & M_2 \end{pmatrix}. \quad (55)$$

In this two-generation scheme we have one CP-violating phase ξ [15]. Although we can start with the same parametrization as in Eq. (47), we have the freedom to change the overall phase of a column or row in m_D without affecting the observables. The change by an overall phase corresponds to a CP transformation of the lepton fields. Multiplying the second column of m_D by $\exp(-i\delta_1 + i\xi)$ and the second row by $\exp(-i\delta_2 + i\xi)$, and taking $\xi = (\delta_1 + \delta_2)/2$, we can get the type of Dirac mass matrix shown in Eq. (55). It is the existence of the left-handed neutral singlet S_L that gives us this freedom to reduce the number of phases.

In order to estimate the tau decays² within Model II, let us find sensible values for the mass parameters. Again, as in Model I, M_1 and M_2 should be of the order of 10^2 GeV or above, to be consistent with the non-observation of heavy neutrinos to date. However, the larger they are, the more suppressed LFV rates will be. Here we take $100 \text{ GeV} \leq M_1 \leq M_2 \leq 1000 \text{ GeV}$.

Concerning the lower mass parameters in the matrix m_D , we should keep in mind that the LFV rates are proportional to $(s_L^{\nu\tau})^2(s_L^{\nu\mu})^2$ or $(s_L^{\nu\tau})^2(s_L^{\nu e})^2$. In turn, these mixings are larger for larger m_D , but the latter cannot be too large, so that bounds in Eq. (42) are still satisfied.

Accordingly, the elements of m_D should be of the order of 10^0 – 10^1 GeV. Here we take first $a = 1$ GeV, $b = c = d = 10$ GeV as representative values. This set of values gives $(s_L^{\nu\tau})^2 \equiv \sum_{h=3}^6 |B_{\tau h}|^2 \approx 0.01$, which is not very sensitive to the value of M_2 , and $(s_L^{\nu e})^2 = \sum_{h=3}^6 |B_{eh}|^2 \approx 0.007$ at $M_2 \approx 120$ GeV, decreasing as M_2 increases. We have plotted the branching ratios for $\tau \rightarrow e\gamma$ (solid line) and $\tau \rightarrow 3e$ (dashed line) as functions of M_2 in Figs. 4. Figs. 4(a), (b), (c) and (d) correspond to the cases $\xi = 0, \pi/4, \pi/2$ and $3\pi/4$, respectively. Fig. 4(b) and Fig. 4(d) show that the branching ratios for $\xi = \pi/4$ have almost the same values as those for $\xi = 3\pi/4$. The branching ratios are maximally reduced when $\xi = \pi/2$, compared to $\xi = 0$ while keeping the same values for the other parameters. At around $M_2 = 500$ GeV the branching ratios for tau decay in Fig. 4(c) show a peculiar behavior: the amplitude for $\tau \rightarrow e\gamma$ changes sign as M_2 varies around that value. The exact value of M_2 at which the decay rate for $\tau \rightarrow e\gamma$ vanishes depends on the other parameters of the model. This behavior is due to quantum interference between the loop diagrams. Fig. 5 shows the T-odd asymmetry A_T as a function of M_2 for $\xi = \pi/4$ (solid line) and $\xi = 3\pi/4$ (dashed line). When all four heavy Majorana neutrinos are degenerate, there is no CP violation [15] and $A_T = 0$. Also $A_T = 0$ if $\xi = \pi/2$.

² In the same way we can analyze muon decays, which have a much lower experimental upper bound than tau decays. To obey the experimental constraints, we need to take a bit smaller values for the parameters a, b, c and d than those we use for tau decays.

The parameters in Model II are not affected by the experimental upper bound of 3 eV on the masses of the three light neutrinos, since the light neutrinos in this model are actually massless. Therefore, the light neutrino mass bounds are irrelevant to our results, as are the requirements of the maximal ($\nu_\mu - \nu_\tau$, $\nu_e - \nu_\mu$) or minimal ($\nu_e - \nu_\tau$ mixing. However, it is well known that many puzzles from the solar and atmospheric neutrino experiments, as well as from cosmology, can be solved by simple interpretation of the effects as neutrino oscillations and eV scale neutrino masses. We could easily produce light neutrino masses in Model II to accommodate neutrino oscillation experiments. For example, the introduction of small Majorana mass terms for the neutral singlets S_{Li} results in non-zero—as well as non-degenerate—masses of the light neutrinos, thus giving us the possibility to easily accommodate Δm_{atm}^2 without significantly affecting the presented LFV rates.

The branching ratios for $\tau \rightarrow e\gamma$ or $\tau \rightarrow 3e$ in Model II are in general significantly larger than those predicted in Model I. Notice however that the $\tau \rightarrow \mu$ rates are more constrained, due to a mixing coefficient $(s_L^{\nu_\mu})^2$ that is an order of magnitude smaller than the corresponding one in $\tau \rightarrow e$ decays [cf. Eq. (42)].

One may ask why our choice of $a = 1$ GeV, $b = c = d = 10$ GeV, is reasonably representative. Indeed, one may alternatively not choose these values, but explore ranges of these Dirac parameters in Model II where the resulting LFV branching ratios, at fixed Majorana masses M_1 and M_2 , are maximal. This is obtained when the inequality (B.3) in the Appendix becomes equality, and the values of the mixing parameters $(s_L)^2$ are maximized, i.e., saturated according to (42). In the case of no CP violation ($\xi = 0$), and, e.g., for the $\nu_e - \nu_\tau$ scenario, the requirement (B.4) for the inequality (B.3) in the Appendix becoming equality gives us the relation $ad = bc$, while the saturation of the values of $(s_L^{\nu_\tau})^2$ and $(s_L^{\nu_e})^2$ gives us two other conditions, for the four Dirac parameters a, b, c, d . This still allows us the freedom of fixing one of the four Dirac parameters. We can, for example, require the symmetry of the (real) m_D matrix: $b = c$. This then results in the following approximately “optimized” choice of m_D parameters (when $\xi = 0$):

$$a = \frac{M_2}{\sqrt{(M_2/M_1)^2 + (s_{2m}/s_{1m})^2}} \frac{s_{1m}}{\sqrt{1 - s_{1m}^2 - s_{2m}^2}}, \quad (56)$$

$$b = c = a \times (s_{2m}/s_{1m}), \quad d = a \times (s_{2m}/s_{1m})^2, \quad (57)$$

where $s_{1m}^2 = (s_L^{\nu_e})_{\max}^2 = 0.0071$ and $s_{2m}^2 = (s_L^{\nu_\tau})_{\max}^2 = 0.033$, according to the bounds (42). If we fix $M_1 = 100$ GeV, the above values of a, b, c, d become functions of M_2 . In Fig. 6(a) we present the LFV branching ratios for this case. They are now, for any value of M_2 , by a factor of about 4 larger than the maximal values in Fig. 4(a) which are achieved for $M_2 = 100$ GeV. In Figs. 6(b,c,d) the LFV branching ratios are presented when $\xi = \pi/4, \pi/2, 3\pi/4$, respectively, by using the same formulas (56)–(57). With the rise of ξ , the branching ratios decrease; however, the formulas (56)–(57) do not necessarily approximate the maximal values of the branching ratios when $\xi \neq 0$. We see from Fig. 6(a) that the LFV branching ratios in Model II, when $100 \text{ GeV} = M_1 \leq M_2 \leq 1000 \text{ GeV}$, are $Br(\tau \rightarrow e\gamma) \lesssim 10^{-8}$ and $Br(\tau \rightarrow 3e) \lesssim 10^{-9}$, and that these values decrease relatively slowly when the parameters of the Dirac sector $(a, b, c, d; \xi)$ are moved away from the “optimal” values. This contrasts with

the LFV branching ratios in the seesaw Model I. The latter model achieved, for the same range of the Majorana masses $100 \text{ GeV} = M_1 \leq M_2 \leq 1000 \text{ GeV}$, maximal values of only $Br(\tau \rightarrow \mu\gamma) \sim 10^{-10}$ and $Br(\tau \rightarrow 3\mu) \sim 10^{-11}$ (the $\nu_e - \nu_\tau$ and $\nu_e - \nu_\mu$ scenarios in Model I gave even smaller values).

The maximal branching ratios in Model II for the $\tau \rightarrow \mu$ LFV processes are suppressed by an additional factor of $(s_L^{\nu_\mu})_{\max}^2 / (s_L^{\nu_e})_{\max}^2 = 0.0014/0.0071 \approx 0.2$ [cf. Eq. (42)]. The maximal branching ratios for the $\mu \rightarrow e$ LFV processes in Model II are suppressed by at least five orders of magnitude, in comparison to the $\tau \rightarrow e$ processes, using a logic similar to that applied in this case to Model I.

While the numerical results in Model II were presented using $M_1 = 100 \text{ GeV}$, the LFV branching ratios increase when M_1 increases and M_2/M_1 , s_{1m} and s_{2m} are kept fixed, a behavior already encountered in Model I. The $Br(\tau \rightarrow 3e)$ increases more significantly than $Br(\tau \rightarrow e\gamma)$ (the latter approaching an asymptotic value). We can thus regard our numerical results in Figs. 4 and 6 as rather conservative values. As a consequence of the aforementioned variation with M_1 , the heavy-to-light mixing parameters needed to result in a given value of a LFV branching ratio decrease when M_1 increases, at fixed M_2/M_1 . This behavior is presented in Figs. 7 and 8, where we plot $(s_L^{\nu_\tau})^2$ as a function of M_1 , keeping $(s_L^{\nu_e})^2$, M_2/M_1 and the branching ratios of $\tau \rightarrow e\gamma$ and $\tau \rightarrow 3e$ as fixed parameters.

C. Expected numbers of events

The explicit numbers of expected events in the considered processes depend on the way the τ leptons are produced and on the luminosities involved. For example, the τ pairs could be produced via $e^+e^- \rightarrow \tau^+\tau^-$ close to the production threshold, or by sitting on a specific vector meson resonance V : $e^+e^- \rightarrow V \rightarrow \tau^+\tau^-$. In the latter case, the production rate $e^+e^- \rightarrow V$ as a function of the CMS energy \sqrt{s} can be approximated as a Breit-Wigner function

$$\sigma(s; e^+e^- \rightarrow V) = K \frac{1}{[(\sqrt{s} - M_V)^2 + (\Gamma_V/2)^2]} , \quad (58)$$

where M_V and Γ_V are the mass and the total decay width of the resonance, respectively. The constant K in Eq. (58) can be fixed by invoking the narrow width approximation (nwa) formula

$$\sigma_{\text{nwa}}(s; e^+e^- \rightarrow V) = \frac{12\pi^2\Gamma_{ee}(V)}{M_V} \delta(s - M_V^2) , \quad (59)$$

where $\Gamma_{ee}(V)$ is the partial decay width for $V \rightarrow e^+e^-$. Namely, the integration of (59) over the variable s gives us $12\pi^2\Gamma_{ee}(V)/M_V$, thus fixing the constant K in the Breit-Wigner form (58): $K = 3\pi\Gamma_{ee}(V)\Gamma_V/M_V^2$. The production cross section is maximal on top of the resonance $\sqrt{s} = M_V$:

$$\begin{aligned}
\sigma(e^+e^- \rightarrow V \rightarrow \tau^+\tau^-)^{\max} &= \sigma(e^+e^- \rightarrow V)^{\max} \times \frac{\Gamma_{\tau\tau}(V)}{\Gamma_V} \\
&\approx 12\pi \frac{\Gamma_{ee}(V)}{\Gamma_V} \frac{\Gamma_{\tau\tau}(V)}{\Gamma_V} \frac{1}{M_V^2}. \tag{60}
\end{aligned}$$

Multiplying this cross section by twice the branching ratio $Br(\tau \rightarrow e\gamma(eee))$ we obtain the cross section for the process $e^+e^- \rightarrow V \rightarrow \tau^+\tau^- \rightarrow e\gamma(eee) + \tau$. These branching ratios are $\lesssim 10^{-8}(10^{-9})$ in Model II, as shown in Figs. 6. For example, if the resonance is taken to be $V = \Upsilon(1S)$ ($M_V = 9.46$ GeV; $\Gamma_{ee}(V)/\Gamma_V \approx \Gamma_{\tau\tau}(V)/\Gamma_V \approx 0.025$), then $\sigma(e^+e^- \rightarrow V \rightarrow \tau^+\tau^- \rightarrow e\gamma(eee) + \tau)$ would be about 2. (0.2) fb. For a luminosity of $10 \text{ fb}^{-1}/\text{yr}$, this corresponds to 20 (2) events per year. Increased luminosities would give correspondingly larger numbers of events.

V. CONCLUSIONS AND SUMMARY

We investigated heavy Majorana neutrino effects on lepton flavor violating (LFV) processes of charged lepton decays, in two seesaw-type models: (I) the interfamily seesaw-type model realized in the SM with right-handed neutrinos, and (II) the SM with left-handed and right-handed neutral singlets. We calculated a T-odd asymmetry, A_T , for charged lepton decays, to test for CP-violating effects under the assumption of CPT conservation. Model I is severely constrained in most of the parameter space for the Dirac mass matrix m_D by the actual eV-scale experimental upper bound on the light neutrino masses. It can give maximal LFV branching ratios $Br(\tau \rightarrow \mu\gamma) \sim 10^{-10}$ and $Br(\tau \rightarrow 3\mu) \sim 10^{-11}$ in a very restricted parameter space where the CP-violating asymmetry A_T is zero, but otherwise it gives branching ratios many orders of magnitude smaller. On the other hand, in Model II the LFV branching ratios can be much larger over a wide range of parameter values, $Br(\tau \rightarrow e\gamma) \sim 10^{-8}$ and $Br(\tau \rightarrow 3e) \sim 10^{-9}$, and A_T can reach values $\sim 10^{-1}$. The results in Model II are insignificantly affected by the experimental bounds on the light neutrino masses. Model II can predict large enough branching ratios to be tested with near future experiments.

ACKNOWLEDGMENTS

The work of G.C. and C.D. was supported by FONDECYT (Chile), Grant No. 1010094 and 8000017, respectively. The work of C.S.K. was supported in part by CHEP-SRC Program and Grant No. 20015-111-02-2, R03-2001-00010 of the KOSEF, in part by BK21 Program and Grant No. 2001-042-D00022 of the KRF, and in part by Yonsei Research Fund, Project No. 2001-1-0057. The work of J.D.K was supported by the Korea Research

Foundation Grant (2001-042-D00022). G.C. wishes to thank S. Kovalenko for helpful discussions.

Appendix A. DIAGONALIZATION OF A COMPLEX SYMMETRIC MATRIX

For completeness we mention here how to diagonalize a complex symmetric matrix \mathcal{M} [23]. The procedure can be divided in two steps. The first step is to diagonalize a generic complex square matrix by means of two unitary matrices U_1 and U_2 in the form $U_1 \mathcal{M} U_2^\dagger = \mathcal{M}_D$, where \mathcal{M}_D is diagonal, real and with non-negative elements. The second step is to show that, if the matrix \mathcal{M} is symmetric, U_1 and U_2 can be chosen to be equivalent, in the sense that $U_2 = U_1^*$, and consequently $U \mathcal{M} U^T = \mathcal{M}_D$.

In the first step, one easily finds two unitary matrices V_1 and V_2 that diagonalize the hermitian (although generally different) matrices $\mathcal{M}\mathcal{M}^\dagger$ and $\mathcal{M}^\dagger\mathcal{M}$, *i.e.* $V_1 \mathcal{M} \mathcal{M}^\dagger V_1^\dagger = \mathcal{M}_D^2$ and $V_2 \mathcal{M}^\dagger \mathcal{M} V_2^\dagger = \mathcal{M}_D^2$, where \mathcal{M}_D^2 is a diagonal non-negative, real matrix. We now define $\mathcal{M}_B \equiv V_1 \mathcal{M} V_2^\dagger$, which is still a complex matrix. However, to obtain $\mathcal{M}_D \equiv U_1 \mathcal{M} U_2^\dagger$, one can show that the required unitary matrices U_i are related to V_i via $V_i = K_i U_i$ ($i = 1, 2$), where K_i are block-diagonal unitary matrices that commute with \mathcal{M}_D :

$$\mathcal{M}_D = \begin{bmatrix} 0 \times I_{n_0} & 0 & \cdots & 0 \\ 0 & m_1 I_{n_1} & \cdots & 0 \\ \vdots & \vdots & \cdots & 0 \\ 0 & 0 & \cdots & m_k I_{n_k} \end{bmatrix}; \quad K_i = \begin{bmatrix} K_i^{(0)} & 0 & \cdots & 0 \\ 0 & K_i^{(1)} & \cdots & 0 \\ \vdots & \vdots & \cdots & 0 \\ 0 & 0 & \cdots & K_i^{(k)} \end{bmatrix}. \quad (\text{A.1})$$

Here, the dimension of the unitary blocks $K_i^{(j)}$ is n_j . Without loss of generality we can take $K_1 = I$, so that $\mathcal{M}_B = K_1 \mathcal{M}_D K_2^\dagger = \mathcal{M}_D K_2^\dagger$. We then take $K_2^\dagger = \mathcal{M}_D'^{-1} \mathcal{M}_B'$, where $\mathcal{M}_D'^{-1}$ is defined as a diagonal matrix whose diagonal elements are the inverse of those of \mathcal{M}_D , except when the latter are zero in which case we take them as 1 in $\mathcal{M}_D'^{-1}$. The matrix \mathcal{M}_B' is equal to \mathcal{M}_B , with the exception of the first $n_0 \times n_0$ block which is taken to be I_{n_0} instead of 0_{n_0} . We can then directly check that the two unitary matrices $U_1 = V_1$ and $U_2 = K_2^\dagger V_2$ transform \mathcal{M} into the real diagonal matrix $\mathcal{M}_D = U_1 \mathcal{M} U_2^\dagger$.

The second step is to find a single unitary matrix U such that $U \mathcal{M} U^T = \mathcal{M}_D$, given that \mathcal{M} is (complex) symmetric. One can show that, in this case, the unitary matrices U_i found above are related as $U_2 = K \times U_1^*$, where $K (= U_2 U_1^T)$ is a block-diagonal unitary and symmetric matrix that commutes with \mathcal{M}_D . A unitary and symmetric matrix can be diagonalized with a real orthogonal matrix O : $K = O^T K_d O$. We then define the square root of K as $K^{1/2} = O^T K_d^{1/2} O$ with the eigenvectors in the matrix O conveniently ordered so that $K^{1/2}$ commutes with \mathcal{M}_D . Then $U = (K^{1/2})^\dagger U_1$ satisfies $U \mathcal{M} U^T = \mathcal{M}_D$.

Appendix B. APPROXIMATE MAXIMIZATION OF THE BRANCHING RATIOS

The amplitude squared for the $l \rightarrow l'\gamma$ LFV process is, according to Eq. (9), approximately proportional to

$$|A|^2 \propto \left| \sum_{\ell=1}^{N_L} B_{\ell\ell}^* B_{\ell'\ell} \times f(0) + \sum_{h=N_L+1}^{N_L+\tilde{N}_R} B_{lh}^* B_{l'h} \times f(m_h^2) \right|^2, \quad (\text{B.1})$$

where the first sum runs over the light, practically massless, intermediate neutrinos, and the second sum over the heavy neutrinos with masses m_h ($\sim M_1 \sim M_2$). The function f depends of the mass of the exchanged neutrino; in the specific case, it is the loop function (14). We now approximate the second sum by assuming that all the heavy neutrinos eigenmasses m_h are the same: $m_h = M$. Then this implies, together with the unitarity of the matrix U (note: $B_{li} = U_{il}^*$)

$$|A|^2 \propto \left| \sum_{h=N_L+1}^{N_L+\tilde{N}_R} U_{h2} U_{h1}^* \right|^2 \times |f(M^2) - f(0)| \propto \left| \sum_{h=N_L+1}^{N_L+\tilde{N}_R} U_{h2} U_{h1}^* \right|^2. \quad (\text{B.2})$$

Here we denoted the flavor index l of the heavier charged lepton as 2 and the index l' of the lighter one as 1.

The amplitude squared for the $l \rightarrow 3l'$ LFV process is, according to Eqs. (10)–(12) and (20)–(23), more complicated. However, in the leading order in $m_D m_M^{-1}$, and when there is no CP violation (when matrix U is real), it is straightforward to show that $|A|^2$ is proportional to the same kind of combination (B.1). Thus, the proportionality (B.2) is approximately satisfied also for the $l \rightarrow 3l'$ LFV process.

The above proportionality can be supplemented by the Schwarz inequality

$$|A|^2 \propto \left| \sum_h U_{h2} U_{h1}^* \right|^2 \leq \sum_h |U_{h2}|^2 \times \sum_{h'} |U_{h'1}|^2 \equiv (s_L^{\nu_2})^2 (s_L^{\nu_1})^2. \quad (\text{B.3})$$

The equality is achieved only when there is a proportionality:

$$\left. \frac{U_{h2}}{U_{h1}} \right|_{h=N_L+1} = \left. \frac{U_{h2}}{U_{h1}} \right|_{h=N_L+2} = \dots = \left. \frac{U_{h2}}{U_{h1}} \right|_{h=N_L+\tilde{N}_R} \quad (\text{B.4})$$

Thus, the approximate maximal value of $|A|^2$, and thus of the LFV branching ratios, is achieved when the values of the heavy-to-light mixing parameters $(s_L^{\nu_2})^2$ and $(s_L^{\nu_1})^2$ are saturated according to the upper bounds (42) and, at the same time, the mixing matrix U elements in the heavy-to-light sector satisfy the equalities (B.4).

In the seesaw Model I (with $N_L = \tilde{N}_R = 2$), the mixing matrix U elements in the heavy-to-light sector are $U_{h2} = (m_M^{-1} m_D^\dagger)_{h'2}$ and $U_{h1} = (m_M^{-1} m_D^\dagger)_{h'1}$, where $h' \equiv h-2$. In our specific case of maximal mixing ($a = c$, $b = -d$, $\delta_1 = \delta_2 = \pi/2$) we have: $U_{31} = a/M_1$, $U_{41} = -ib/M_2$, $U_{32} = -ia/M_1$, $U_{42} = -b/M_2$; the equality (B.4) is fulfilled; and $(s_L^{\nu_1})^2 = (s_L^{\nu_2})^2 = (a^2/M_1^2 + b^2/M_2^2)$.

In Model II (with $N_L = 2$ and $\tilde{N}_R = 4$), with $\xi = 0$, it can be shown, e.g. by using *Mathematica*, that the equality (B.4) is satisfied when $ad = bc$. If in this case also the values of $(s_L^{\nu_2})^2 = \sum_h |U_{h2}|^2$ and $(s_L^{\nu_1})^2 = \sum_h |U_{h1}|^2$ are saturated by the corresponding upper bounds of Eq. (42), then the approximate maximal branching LFV ratios are achieved.

REFERENCES

- [1] T. Yanagida, *Proceedings of the Workshop on Unified Theory and Baryon Number of the Universe*, eds. O. Swada and A. Sugamoto (KEK, 1979) p.95; M. Gell-Mann, P. Ramond and R. Slansky, *Supergravity*, eds. P. van Nieuwenhuizen and D. Friedman (North-Holland, Amsterdam, 1979) p. 315; R. N. Mohapatra and G. Senjanović, Phys. Rev. Lett. **44**, 912 (1980).
- [2] E. Witten, Nucl. Phys. B **268**, 79 (1986); R. N. Mohapatra and J. W. Valle, Phys. Rev. D **34**, 1642 (1986); J. L. Hewett and T. G. Rizzo, Phys. Rept. **183** (1989) 193.
- [3] D. Wyler and L. Wolfenstein, Nucl. Phys. B **218**, 205 (1983).
- [4] A. Ilakovac and A. Pilaftsis, Nucl. Phys. B **437**, 491 (1995) [arXiv:hep-ph/9403398].
- [5] J. G. Körner, A. Pilaftsis and K. Schilcher, Phys. Rev. D **47**, 1080 (1993) [arXiv:hep-ph/9301289].
- [6] M. C. Gonzalez-Garcia and J. W. Valle, Mod. Phys. Lett. A **7**, 477 (1992).
- [7] Y. Okada, K. i. Okumura and Y. Shimizu, Phys. Rev. D **58**, 051901 (1998) [arXiv:hep-ph/9708446]; *ibid.* **61**, 094001 (2000) [arXiv:hep-ph/9906446].
- [8] C. Dib, V. Gribanov, S. Kovalenko and I. Schmidt, Talk given at International Workshop on Neutrinos and Physics Beyond the Standard Model NANPino (Non-Accelerator New Physics in Neutrino Observations), Dubna, Moscow region, Russia, 19-22 Jul 2000, [arXiv:hep-ph/0011213].
- [9] F. del Aguila, E. Laermann and P. Zerwas, Nucl. Phys. B **297**, 1 (1988); E. Ma and J. Pantaleone, Phys. Rev. D **40**, 2172 (1989); J. Kogo and S. Y. Tsai, Prog. Theor. Phys. **86**, 183 (1991); W. Buchmüller and C. Greub, Nucl. Phys. B 363 (1991) 345; *ibid* 381 (1992) 109; J. Maalampi, K. Mursula, and R. Vuopionperä, Nucl. Phys. B 372 (1992) 23; A. Datta and A. Pilaftsis, Phys. Lett. B **278**, 162 (1992). A. Datta, M. Guchait and A. Pilaftsis, Phys. Rev. D **50**, 3195 (1994) [arXiv:hep-ph/9311257]; J. Gluza and M. Zrałek, Phys. Rev. D **48** (1993) 5093; *ibid* **51**, 4695 (1995) [arXiv:hep-ph/9409225]; *ibid* **51**, 4707 (1995) [arXiv:hep-ph/9409224]; A. Hofer and L. M. Sehgal, Phys. Rev. D **54**, 1944 (1996) [arXiv:hep-ph/9603240]; G. Cvetič, C. S. Kim and C. W. Kim, Phys. Rev. Lett. **82**, 4761 (1999) [arXiv:hep-ph/9812525]; G. Cvetič and C. S. Kim, Phys. Lett. B **461**, 248 (1999), *ibid* **B471** (2000) 471E [arXiv:hep-ph/9906253]; F. M. Almeida, Y. A. Coutinho, J. A. Martins Simoes and M. A. do Vale, Phys. Lett. B **494**, 273 (2000) [arXiv:hep-ph/0008231]; hep-ph/0101077;
- [10] M. Flanz, W. Rodejohann and K. Zuber, Eur. Phys. J. C **16**, 453 (2000) [arXiv:hep-ph/9907203]; K. Zuber, Phys. Lett. B **479**, 33 (2000) [arXiv:hep-ph/0003160]; W. Rodejohann and K. Zuber, Phys. Rev. D **62**, 094017 (2000) [arXiv:hep-ph/0005270]; C. Dib, V. Gribanov, S. Kovalenko and I. Schmidt, Phys. Lett. B **493**, 82 (2000) [arXiv:hep-ph/0006277].
- [11] A. Kageyama, S. Kaneko, N. Shimoyama and M. Tanimoto, Phys. Lett. B **527**, 206 (2002) [arXiv:hep-ph/0110283]; A. Kageyama, S. Kaneko, N. Shimoyama and M. Tanimoto, arXiv:hep-ph/0112359, and references therein.
- [12] G. Cvetič, M. Nowakowski and A. Pilaftsis, Phys. Lett. B **301**, 77 (1993) [arXiv:hep-ph/9301272]; G. Cvetič, Phys. Rev. D **48**, 5280 (1993) [arXiv:hep-ph/9309202].
- [13] T. Endoh, T. Morozumi, T. Onogi and A. Purwanto, Phys. Rev. D **64**, 013006 (2001) [arXiv:hep-ph/0012345].

- [14] J. F. Nieves and P. B. Pal, Phys. Rev. D **64**, 076005 (2001) [arXiv:hep-ph/0105305].
- [15] G. C. Branco, M. N. Rebelo and J. W. F. Valle, Phys. Lett. B **225**, 385 (1989).
- [16] M. C. Gonzalez-Garcia and J. W. Valle, Phys. Lett. B **216**, 360 (1989).
- [17] J. Hisano and K. Tobe, Phys. Lett. B **510**, 197 (2001) [arXiv:hep-ph/0102315].
- [18] S. K. Kang and C. S. Kim, Phys. Rev. D **63**, 113010 (2001) [arXiv:hep-ph/0012046];
K. S. Kang, S. K. Kang, C. S. Kim and S. M. Kim, Mod. Phys. Lett. A **16**, 2169 (2001) [arXiv:hep-ph/9808419].
- [19] P. Langacker and D. London, Phys. Rev. D **38**, 886 (1988).
- [20] E. Nardi, E. Roulet and D. Tommasini, Phys. Lett. B **327**, 319 (1994) [arXiv:hep-ph/9402224].
- [21] D. E. Groom *et al.* [Particle Data Group Collaboration], Eur. Phys. J. C **15**, 1 (2000).
- [22] V. Barger, S. Pakvasa, T.J. Weiler and K. Whisnant, Phys. Lett. B **437**, 107 (1998);
H. Georgi and S.L. Glashow, Phys. Rev. D **61**, 097301 (2000); M. Jezabek and Y. Sumino, Phys. Lett. B **457**, 139 (1999); C.H. Albright and S.M. Barr, Phys. Rev. D **61**, 035009 (2000); S. K. Kang and C. S. Kim, Phys. Rev. D **59**, 091302 (1999) [arXiv:hep-ph/9811379]; C. S. Kim and J. D. Kim, Phys. Rev. D **61**, 057302 (2000) [arXiv:hep-ph/9908435].
- [23] J. Bernabeu and P. Pascual, Nucl. Phys. B **228**, 21 (1983); J. A. Aguilar-Saavedra, Int. J. Mod. Phys. C **8**, 147 (1997) [arXiv:hep-ph/9607313].

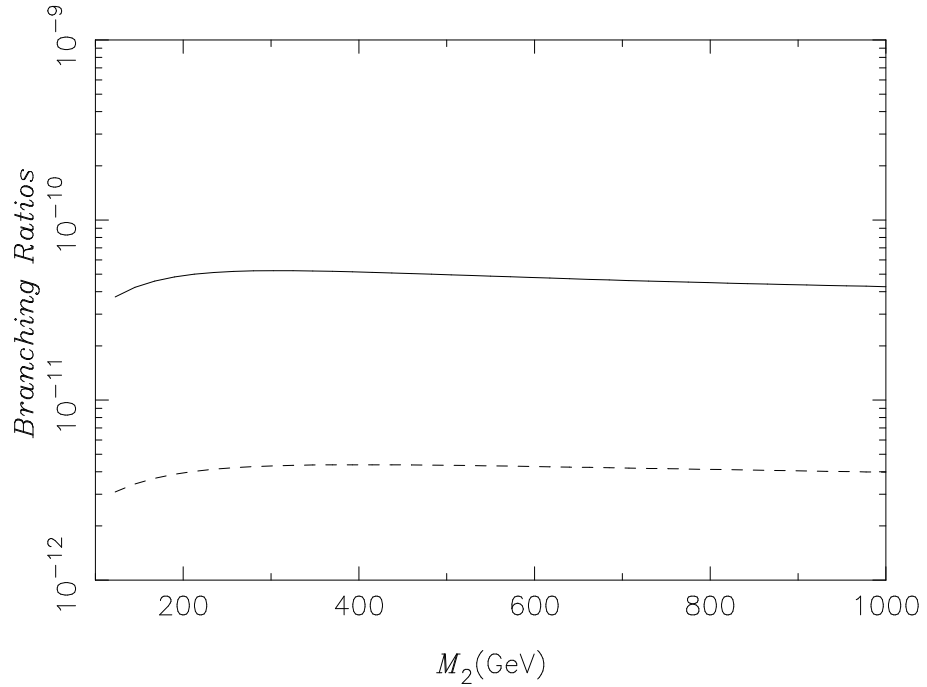


FIG. 1. Branching ratios for $\tau \rightarrow \mu\gamma$ (solid line) and $\tau \rightarrow 3\mu$ (dashed line) as functions of M_2 in Model I: we set $M_1 = 100$ GeV and the other parameters are chosen in the form (53)–(54) which give maximal branching ratios when $\delta_1 = \delta_2 \equiv \delta = \pi/2$.

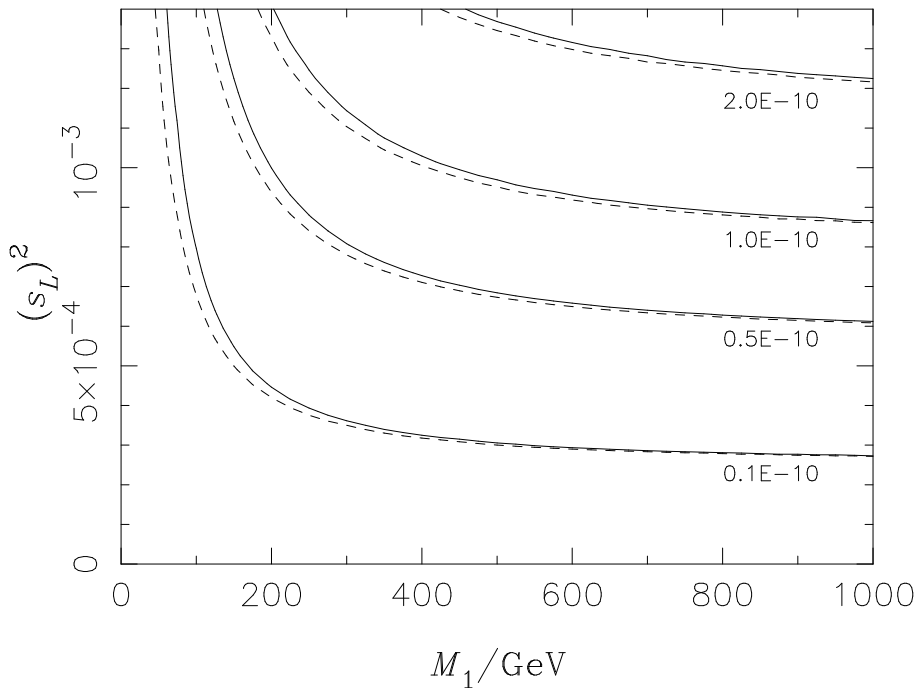


FIG. 2. Mixing parameter s_L^2 ($= (s_L^{\nu\mu})^2 = (s_L^{\nu\tau})^2$) as a function of M_1 in Model I, for various values of $Br(\tau \rightarrow \mu\gamma)$, when $M_2/M_1 = 1$ (solid line) and $M_2/M_1 = 10$ (dashed line). We set the Dirac parameters (a, b, c, d) in the form (53)–(54), with $\delta_1 = \delta_2 \equiv \delta = \pi/2$ and $(s_L)_{\max} \mapsto s_L$. The maximal (s_L^2) is 0.0014, according to (42).

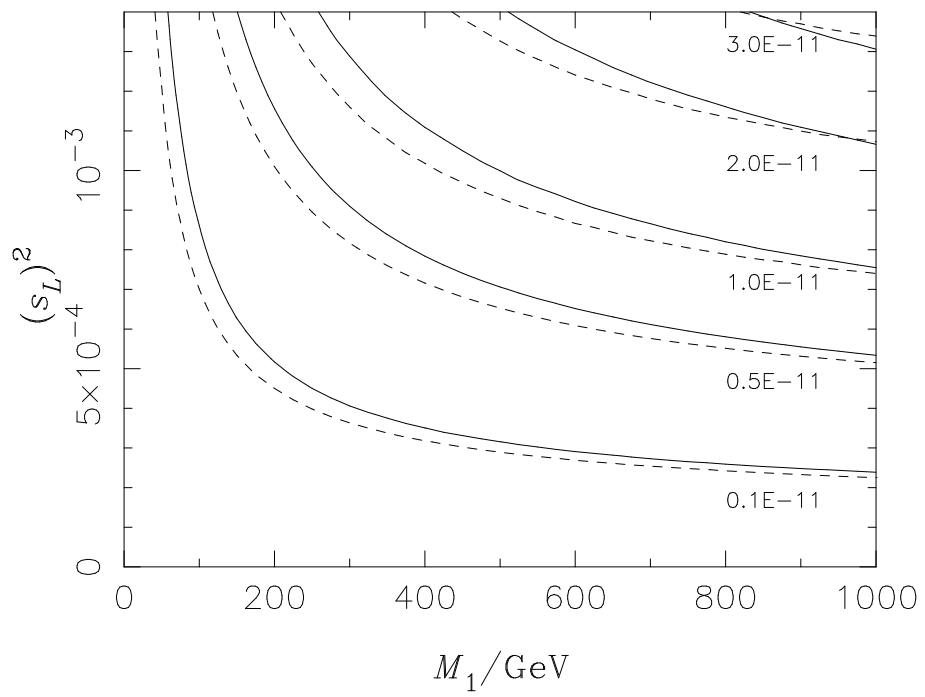


FIG. 3. Same as in Fig. 2, but this time for various fixed values of $\text{Br}(\tau \rightarrow 3\mu)$.

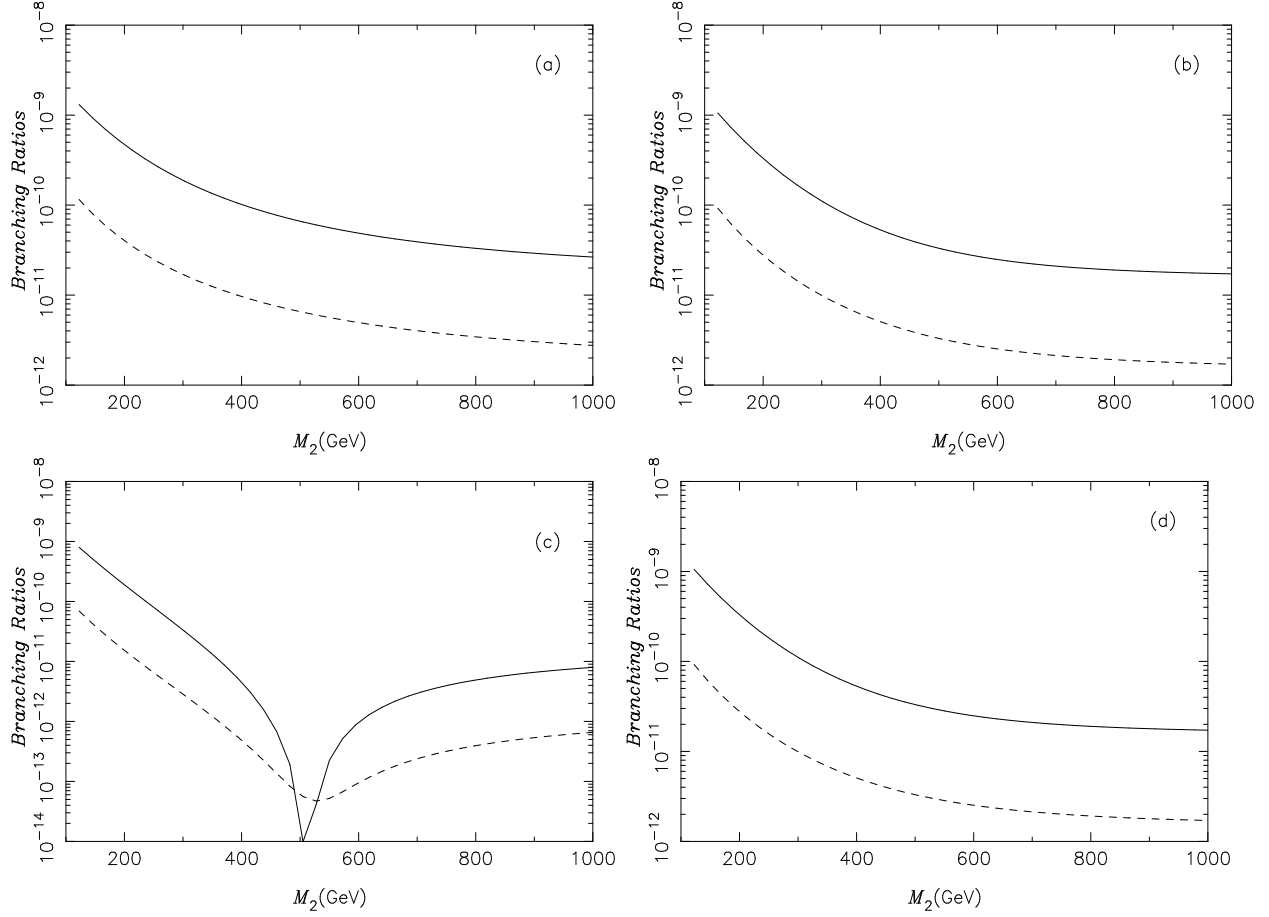


FIG. 4. Branching ratios for $\tau \rightarrow e\gamma$ (solid line) and $\tau \rightarrow 3e$ (dashed line) as functions of M_2 in Model II: the parameters in the mass matrix are $a = 1$ GeV, $b = c = d = 10$ GeV, $M_1 = 100$ GeV, and the CP-violating phase is (a) $\xi = 0$, (b) $\xi = \pi/4$, (c) $\xi = \pi/2$, and (d) $\xi = 3\pi/4$.

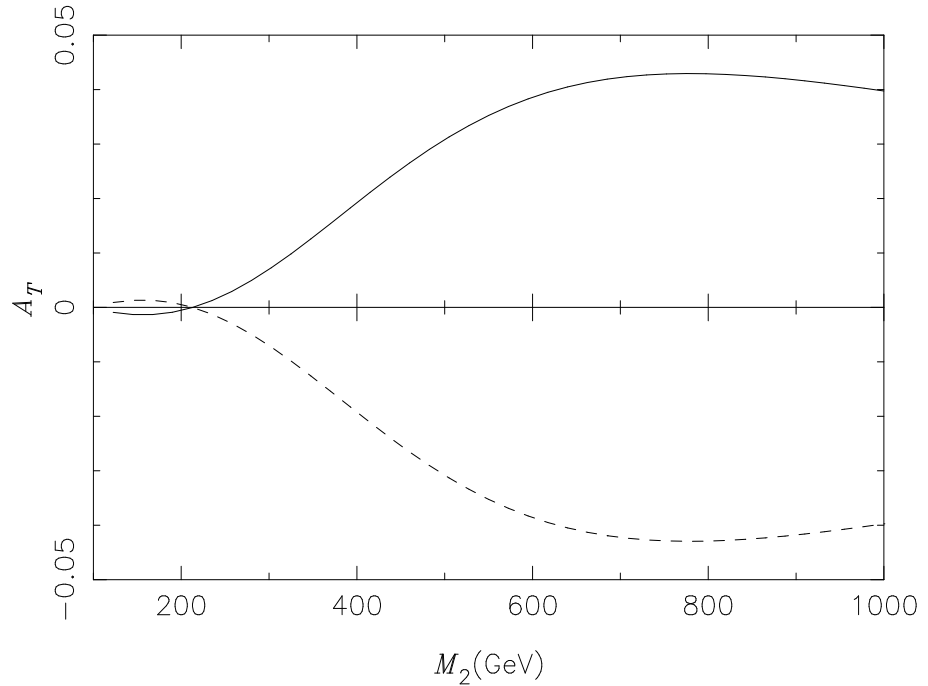


FIG. 5. The T-asymmetry A_T for the decay $\tau \rightarrow eee$ as a function of M_2 with $\xi = \pi/4$ (solid line) and $\xi = 3\pi/4$ (dashed line) in Model II. $A_T = 0$ at $\xi = \pi/2$. Other parameters are the same as those for Fig. 1.

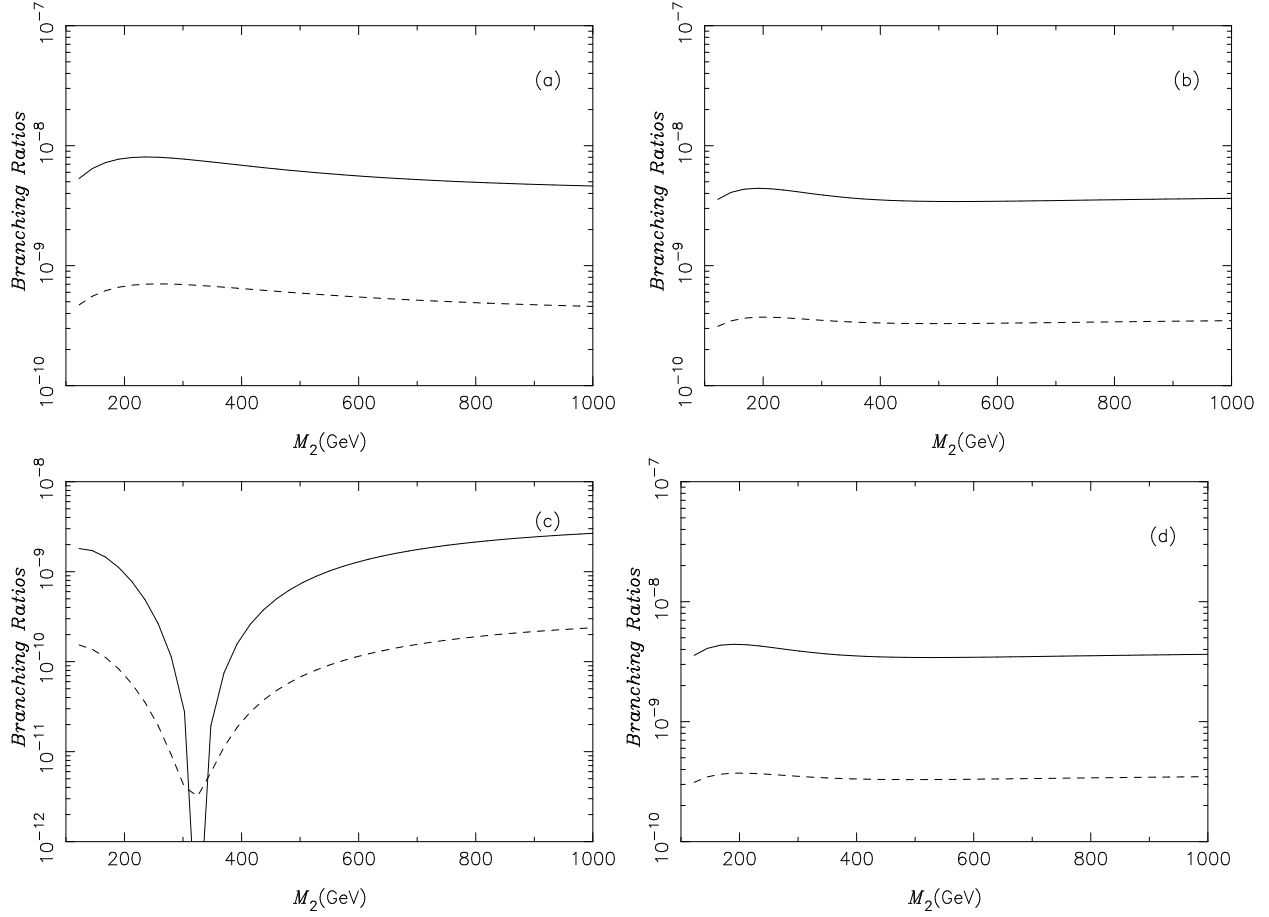


FIG. 6. Branching ratios for $\tau \rightarrow e\gamma$ (solid line) and $\tau \rightarrow 3e$ (dashed line) as functions of M_2 , at fixed $M_1 = 100$ GeV, in Model II: the parameters a, b, c, d in the Dirac mass matrix m_D are chosen in the form (56)–(57) which give approximately maximal branching ratios when $\xi = 0$ (a). Displayed are also the results when $\xi = \pi/4$ (b), $\xi = \pi/2$ (c), and $\xi = 3\pi/4$ (d), with the same a, b, c, d .

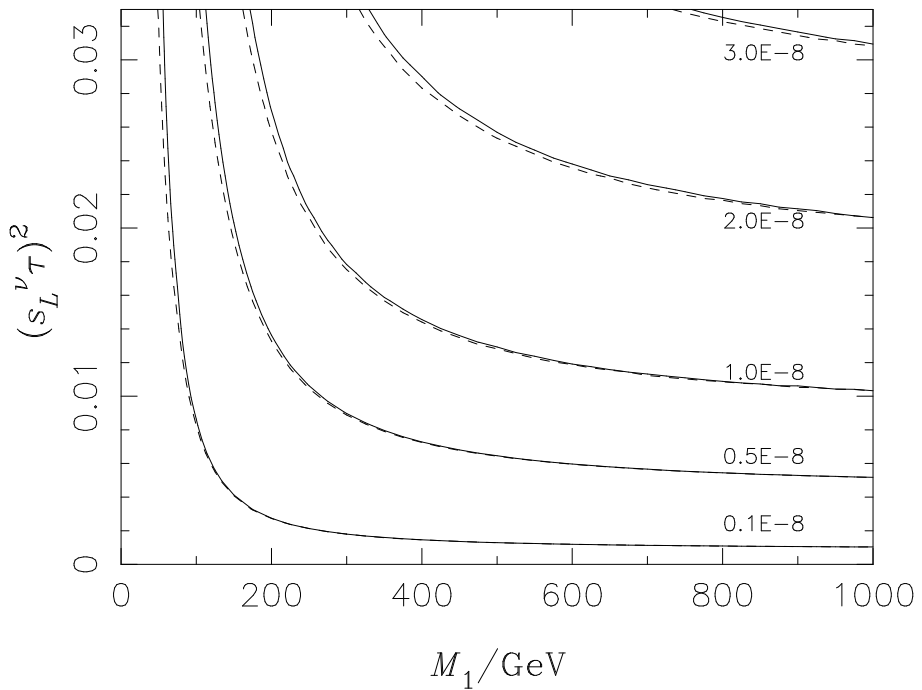


FIG. 7. Mixing parameter $(s_L^{\nu\tau})^2$ as a function of M_1 in Model II, for various fixed values of $Br(\tau \rightarrow e\gamma)$, when $M_2/M_1 = 1$ (solid line) and $M_2/M_1 = 10$ (dashed line). We set $\xi = 0$ and the Dirac parameters (a, b, c, d) in the form (56)–(57), with $s_{1m}^2 = (s_L^{\nu e})_{\max}^2 = 0.0071$ [cf. Eq. (42)] and $s_{2m} \mapsto s_L^{\nu\tau}$. The maximal value of $(s_L^{\nu\tau})^2$ is 0.033, according to (42).

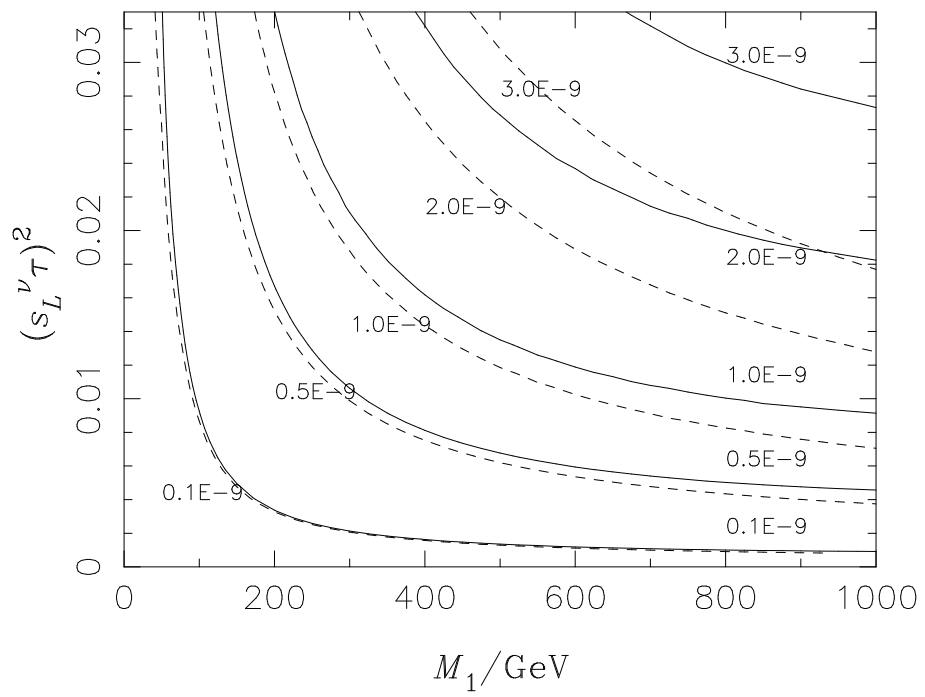


FIG. 8. Same as in Fig. 7, but this time for various fixed values of $Br(\tau \rightarrow 3e)$.